The Two-Component System CCl_4 + $CBrCl_3$. Inference of the Lattice Symmetry of Phase II of $CBrCl_3$

María Barrio,[†] Luis C. Pardo,[†] Josep Ll. Tamarit,*[,†] Philippe Negrier,[‡] David O. López,[†] Josep Salud,[†] and Denise Mondieig[‡]

Departament de Física i Enginyeria Nuclear, ETSEIB, Universitat Politècnica de Catalunya, Diagonal, 647 08028 Barcelona, Catalonia, Spain, and Centre de Physique Moléculaire, Optique et Hertzienne, UMR 5798 au CNRS-Université Bordeaux I, 351, cours de la Libération, 33405 Talence Cedex, France

Received: April 2, 2004; In Final Form: May 13, 2004

The phase diagram of the two-component system between two halomethanes, carbon tetrachloride (CCl_4) and bromotrichloromethane ($CBrCl_3$) has been determined by means of X-ray powder diffraction and thermal analysis techniques from 200 K to the liquid state. From the continuous series of mixed crystals, three relations of isomorphism have been evidenced: (i) between the stable low-temperature monoclinic (M) phases, (ii) between the stable orientationally disordered (OD) rhombohedral (R) phases, and (iii) between the stable OD face-centered cubic (FCC) of $CBrCl_3$ and the metastable FCC phase of CCl_4. The existence of such a metastable phase gives rise to the appearance, for a large range of composition, of metastable FCC mixed crystals that behave monotropically with respect to the R mixed crystals accordingly with the well-known monotropic character of the R to FCC phase transition of the CCl_4. The isomorphism relationships i and ii enable us to validate the previously proposed structure of the monoclinic phase of $CBrCl_3$ ($C2/c$, $Z = 32$) and to determine the lattice symmetry of the OD rhombohedral phase (relation ii) of $CBrCl_3$, the symmetry of which is the same as that of the R phase of CCl_4, respectively. The thermodynamic assessment reproduces coherently the phase diagram (stable two-phase equilibria, M + R, R + L, and a part of the FCC + L) as well as the partially metastable [FCC + L] two-phase equilibrium and provides a coherent set of data for the thermodynamic properties of nonexperimentally available phase transitions of pure components.

Introduction

Among many highly symmetrical molecules displaying an orientationally disordered (OD) high-temperature solid phase in which more or less hindered rotation exists, the tetrahalogenomethane (CX_nY_m, where n and $m = 0, ..., 4$, $n + m = 4$, and X and Y = F, Cl, Br, and I) have seemed to offer an exceptionally good opportunity for the analysis of the steric and intermolecular interactions controlling phase behavior.[1−4] It was identified early for many of these materials that the dipole−dipole (or induced-dipole) interactions are not sufficient to prevent orientational molecular disorder in the solid state.[1,2] Nevertheless, despite the large molecular structure similarity, the polymorphic behavior of these materials has not been rationalized into a common scheme. As for two of the tetrahalogenomethanes dealt within this paper, carbon tetrachloride, CCl_4, and bromotrichloromethane, $CBrCl_3$, two apparently different phase sequences have been described. Although compounds exhibiting OD phases (currently called plastic crystals)[5] often exhibit only one disordered phase, $CBrCl_3$ has long been known to form, in addition to the high-temperature face-centered cubic (FCC) phase I an additional OD phase (II) prior to forming the low-temperature phase (III).[1,6−8] Both III−II and II−I phase transitions are known to be reversible.[6] The situation is sketched in Figure 1a, where the molar Gibbs energies as a function of temperature are plotted for the OD and liquid phases.

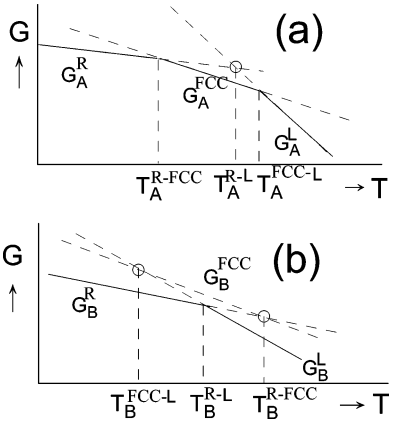

Figure 1. Gibbs energy vs temperature diagrams for pure substance B displaying two polymorphs (R and FCC) with enantiotropic behavior (a) and for pure substance A for which FCC form, invariably, is metastable with respect to R, and the kind of polymorphism is referred to as monotropism (b). Dashed Gibbs curves reflect metastability and open circles metastable points.

The thermodynamic properties for two tetrahalogenomethane compounds of the series $CBr_{4-n}Cl_n$ ($n = 0, ..., 4$), particularly for $n = 2$ (CBr_2Cl_2) and $n = 3$ ($CBrCl_3$), were determined by means of adiabatic calorimetry.[6] One of the main conclusions of this work, in addition to the establishment of the stable polymorphic behavior of both compounds, was the existence of a glass transition (at ca. 90 K) at which, according to the measured excess entropy around the singularity, the molecular motion frozen in was assigned to the exchange of the Cl and Br atoms. The nomenclature used for identifying polymorphic

* To whom correspondence may be addressed. Phone: +34 93 401 65 64. Fax +34 93 401 18 39. E-mail: jose.luis.tamarit@upc.es.
[†] Universitat Politècnica de Catalunya.
[‡] CNRS-Université Bordeaux.

10.1021/jp048553+ CCC: $27.50
Published on Web 06/22/2004

solid phases in the above-mentioned work (Ia for the FCC OD phase and Ib for the R OD phase) deserves a special comment in order to avoid a source of inconsistency in the literature. In OD phases, it is commonly accepted to label the phase formed before melting as phase I and succeeding phases with decreasing temperature as phases II, III, and so on. Nevertheless, when one of these phases displays a monotropic behavior (Figure 1b, as we will see for CCl_4) it has been usually accepted to differentiate the phases formed before the multiple melting processes as Ia, Ib, etc.[9,10] Because phase transitions between the OD phases of $CBrCl_3$ are reversible (enantiotropic behavior), we will use the accepted nomenclature.

Binbrek et al.[7] described the structure of the phase III of $CBrCl_3$, from neutron powder diffraction, in terms of the $C2/c$ space group with $Z = 32$, which is isostructural to all four members of the CCl_nBr_{4-n} ($n = 0$, ..., 4) family.[7,11−17] For the low-temperature monoclinic phase of the $n = 2$ and 3 compounds of this family, the molecules were assumed to be disordered so that sites have fractional occupancies of 0.5 for each of the Cl and Br atoms for $n = 2$ and 0.75 and 0.25 for $n = 3$, respectively.[7] The authors of that work did not detect any ordering of the molecules in the low-temperature phase, although such an ordering is expected since each of the four molecules in the asymmetric unit has a distinct surroundings. Nevertheless, it should be noticed that these results agree quite well with the reported excess entropy determined for the glass transition. The authors[7] also identified the unit cell of the high-temperature OD FCC, but attempts to determine the lattice symmetry of the intermediate OD phase II of $CBrCl_3$ were unsuccessful.

As far as CCl_4 is concerned, the polymorphic behavior is slightly different as for $CBrCl_3$ and has been largely described.[11−13,18−23] On cooling from the liquid, it crystallizes to an OD FCC phase, and upon further cooling, it transforms to another rhombohedral (R) phase, which turns to the low-temperature phase (also $C2/c$, $Z = 32$) on further cooling. When cooling is limited such that an FCC phase is formed, this phase melts on heating without passing through the R phase. Similarly, when heated from phase R, a new melting point higher than that of phase FCC is obtained. This indicates that phase FCC is a metastable phase and, consequently, that the FCC−R transition has a monotropic character (see Figure 1b). According to the labeling scheme proposed by Rudman, the metastable FCC phase was called Ia and the stable rhombohedral one Ib.[9,10] The structure of the fully ordered low-temperature phase II was early determined[14] and the lattice symmetries of both the stable and metastable phases were also a long time ago reported by Rudman.[11] Recently, the study of some two-component systems in which CCl_4 was involved has provided more accurate lattice parameters for both OD phases.[24−26]

The current experimental work was undertaken for two purposes: (i) First, we wish to investigate whether the lattice symmetry of the OD phase II of $CBrCl_3$ is isomorphous to that of the OD stable rhombohedral phase of CCl_4 and (ii) second, we wish to establish the links between the OD stable or metastable phases of these compounds within in a more general study of the tetrahalogenated methanes. The two main aims of this work are conducted through the study of the stable and metastable mixed crystals in the OD state of the $CCl_4 + CBrCl_3$ two-component system. In addition, and by the way, the isomorphism between the low-temperature ordered phases is demonstrated.

2. Experimental Section

2.1. Materials. The chemicals CCl_4 and $CBrCl_3$ were obtained from Across with purities of 99+ and 99%, respectively. They were used as received since the measured melting points agreed well with the ones reported earlier.[1,6,8,11,20] Binary mixtures were prepared at room temperature, i.e., in the liquid state, by mixing the materials in the desired proportions.

2.2. Thermal Analysis. Calorimetric measurements were conducted under nitrogen flux using a Perkin-Elmer DSC-7 differential scanning calorimeter equipped with a low-temperature system. Heating and cooling rates of 2 $K \cdot min^{-1}$ were used on sample masses of about 15 mg placed into high-pressure stainless steel pans (also from Perkin-Elmer).

2.3. X-ray Powder Diffraction. X-ray high-resolution diffraction patterns were recorded by means of a horizontally mounted INEL cylindrical position-sensitive detector (CPS 120) using Debye−Scherrer geometry (angular step ca. $0.029°-2\theta$).[27] Monochromatic Cu $K\alpha_1$ ($\lambda = 1.54059$ Å) radiation was selected. Low-temperature measurements were achieved with a liquid nitrogen 600 series Cryostream Cooler from Oxford Cryosystems. The generator power was set to 40 kV and 25 mA. Liquid samples were placed into 0.3 mm diameter Lindemann capillaries which rotate around their long axes during data collection.

External calibration using the $Na_2Ca_3Al_2F_4$ cubic phase was performed by means of cubic spline fittings.[28] The peak positions were determined by pseudo-Voigt fittings. After the patterns were indexed, lattice parameters were refined by means of the AFMAIL program.[29]

3. Results

3.1. Differential Scanning Calorimetry. The temperatures and enthalpy and entropy changes for the phase transitions of the pure components determined from DSC are gathered in Table 1. Such values match quite well with previously reported values.[6,10,19−22]

From DSC measurements the temperatures of the two-phase equilibria have also been obtained. The mixed crystals $(CCl_4)_{1-X}(CBrCl_3)_X$ have been analyzed as a function of the stable and metastable behavior. To determine the stable phase diagram, samples were cooled from room temperature down to about 203.2 K at 2 $K \cdot min^{-1}$ and heated back to room temperature.

For samples within the $0 \leq X < 0.80$ composition range, three phase transitions occur on cooling while only two occur on heating back to room temperature. According to the X-ray diffraction measurements (described below), transitions on cooling were related to liquid to FCC, FCC to R, and R to the low-temperature monoclinic (M) phase. In contrast, the R mixed crystals do not revert to the FCC mixed crystals on heating back and only M to R and R to liquid transitions were found on heating. When cooling is limited such that only the FCC mixed crystals are formed, they melt on heating, without transformation to the R phase. Such a behavior demonstrates the metastability of the FCC mixed crystals (their melting temperature is below that of the corresponding R mixed crystals) and the irreversibility of the FCC−R transition, i.e., its monotropic character (as it occurs for the pure component CCl_4) in this composition range. In other words, the pattern of Figure 1b for the relative position of the Gibbs curves of the OD phases is fulfilled in this molar range.

From the molar composition of 0.80 and higher, the successive phase transitions appearing on cooling are liquid to FCC, FCC to R, and R to M, all of them being reversible transitions. This evidences the enantiotropic behavior of these phases in this molar range. From the calorimetric results, the temperatures of the stable melting equilibria [R + L] and [FCC + L], the stable equilibrium between the OD phases FCC and R [FCC +

TABLE 1: Temperatures and Enthalpy and Entropy Changes Associated with the Phase Transitions of CCl_4 and $CBrCl_3$ Obtained in This Work and from Previously Reported Adiabatic Calorimetry[a]

	transition	T/K	ΔH/kJ·mol^{-1}	ΔS/J·mol^{-1}·K^{-1}	ref
CCl_4	$M^s \rightarrow R^s$	225.9	4.68	20.72	this work
		225.35	4.581	20.33	22
		225.70 ± 0.01	4.631 ± 0.020	20.52	20
	$R^s \rightarrow L^s$	250.3	2.52	10.06	this work
		250.3	2.515	10.05	22
		250.53 ± 0.01	2.562	10.23	20
	$FCC^m \rightarrow L^s$	245.8	1.82	7.42	this work
		246.01 ± 0.01	1.830 ± 0.070	7.44	20
	$R^m \rightarrow FCC^m$	262.9‡	0.69‡	2.64‡	this work
$CBrCl_3$	$M^s \rightarrow R^s$	238.1	4.58	19.23	this work
		238.19	4.618‡	19.40‡	6
	$R^s \rightarrow FCC^s$	260.3	0.52	1.98	this work
		259.34	0.527	2.03	6
	$FCC^s \rightarrow L^s$	267.1	2.03	7.61	this work
		267.9	2.032	7.59	6
	$R^m \rightarrow L^m$	265.7†	2.55†	9.58†	this work

[a] The stable and metastable transitions are denoted by superscript s and m, respectively. Values obtained from the extrapolation of experimental values are denoted by †, and values obtained from fundamental thermodynamics (see text) are denoted by ‡. M refers to the low-temperature monoclinic ($C2/c$) phase of CCl_4 and $CBrCl_3$, and R and FCC for the OD Phases.

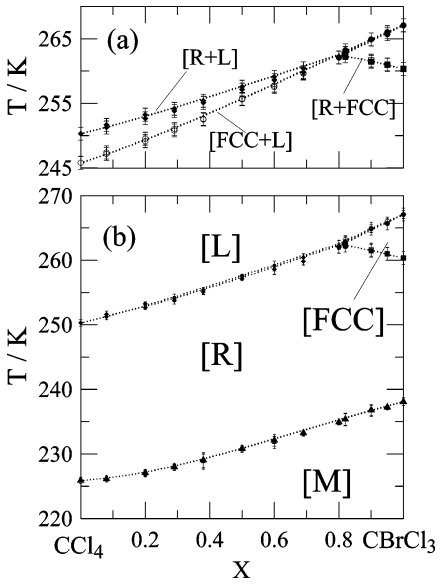

Figure 2. The temperature composition $CCl_4 + CBrCl_3$ phase diagram. (a) Stable (full symbols) and metastable (empty symbols) parts corresponding to the [FCC + L] and [R + L] melting equilibria and (b) stable binary phase diagram obtained by the thermodynamic assessment together with the experimental points.

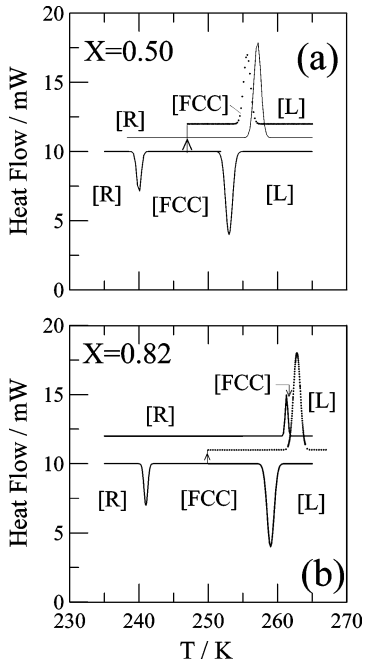

Figure 3. Heating and cooling DSC thermograms for mixed crystals $(CCl_4)_{0.50}(CBrCl_3)_{0.50}$ (a) and $(CCl_4)_{0.18}(CBrCl_3)_{0.82}$ (b) for which FCC and R phases behave monotropically and enantiotropically, respectively.

R], the stable equilibrium between the OD R phase and the low-temperature monoclinic phase [M + R], and the part of the metastable melting equilibrium [FCC + L] have been built up and are plotted in Figure 2, the $T-X$ phase diagram. The two-component system has a peritectic three-phase equilibrium at 262.4 ± 1.0 K sharing FCC, R, and L phases. Two speaking examples of the calorimetric output for mixed crystals crossing melting equilibria for the two composition domains are depicted in Figure 3.

As can be seen from Figure 2, the [FCC + L] melting equilibrium goes continuously from $X = 0$ (CCl_4) to $X = 1$ ($CBrCl_3$), despite being metastable from $X = 0$ to $X \approx 0.8$ (due to the monotropic character of the FCC phase). It is noteworthy that with increasing mole fraction the [R + L] equilibrium would end (at X = 1) at the nonexperimentally available melting temperature of phase R of $CBrCl_3$ (see Figure 1a, T_A^{R-L}) and that on decreasing the mole fraction the [R + FCC] equilibrium would end (at $X = 0$) at the nonexperimentally available R to FCC transition temperature of CCl_4 (see Figure 1b, T_B^{R-FCC}).

DSC measurements contain also information about the heat effect associated with the solid−solid and melting transitions. Figure 4 shows the measured heat effects as a function of composition. According to the described DSC measurements, the enthalpy changes associated with the melting of FCC mixed crystals and the M to R transition were measured continuously for the whole composition range. As far as the melting enthalpy of the R mixed crystals is concerned, direct experimental data are obtained from $X = 0$ to $X \approx 0.80$. Nevertheless, assuming that the specific heat of the FCC and R mixed crystals are close the enthalpy changes between the FCC, R, and L phases can be related by the equation

$$\Delta H_{R\rightarrow L} = \Delta H_{R\rightarrow FCC} + \Delta H_{FCC\rightarrow L} \quad (1)$$

and thus, the melting enthalpy for the R mixed crystals for mole fractions at about 0.80 and higher can be determined. Extrapolation at $X = 1$ of the R to L melting enthalpy values enables to

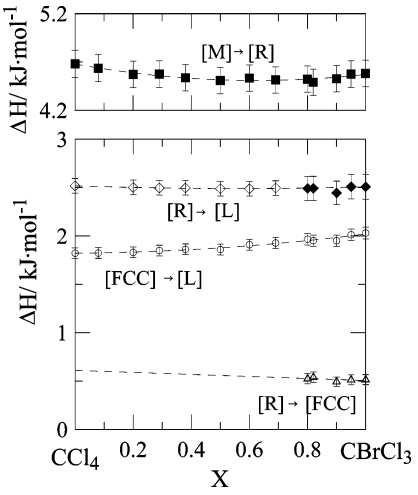

Figure 4. Experimental enthalpies for the monoclinic to R transition (■) of melting for the FCC (○) and (◇,♦) R mixed crystals and enthalpy changes for the R to FCC transition (△) as a function of mole fraction. Full symbols (♦) correspond to the calculated values of the enthalpy of melting of the R mixed crystals for $X \geq 0.8$ according to eq 1 (see text).

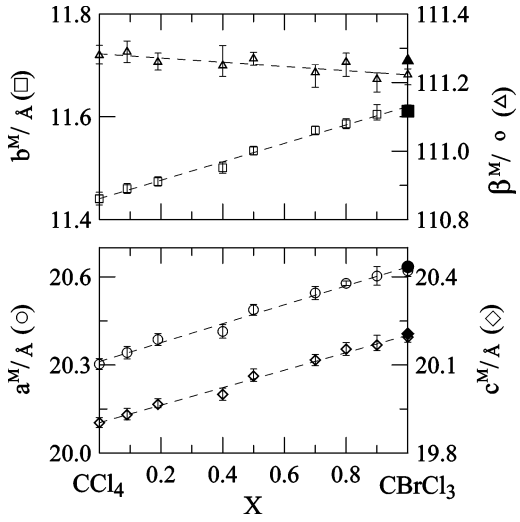

Figure 5. Lattice parameters as a function of the mole fraction for the low-temperature monoclinic mixed crystals at 223.2 K. Full symbols correspond to the lattice parameters at 225 K reported by Binbrek et al.[7]

obtain the enthalpy change associated with the melting of the R phase of $CBrCl_3$. It must be stressed that the difference between such a value (2.509 kJ·mol^{-1}) and that obtained from eq 1 (2.546 kJ·mol^{-1}) is clearly smaller than the uncertainty in the absolute value of the heat effects. Such a result proves the hypothesis used to establish eq 1 and thus the validity of the melting enthalpy values of the R phase for molar compositions ranged between 0.80 and 1.

3.2. Crystallographic Study. To verify the isomorphism relationship between the isostructural phases of the two components (M, R, and FCC), isothermal X-ray powder diffraction studies at different temperatures in the mixed crystals were undertaken at 243.2 and 223.2 K for the OD R and FCC phases and for the low-temperature monoclinic phase, respectively. Moreover, these studies enable us to analyze the variation of the lattice parameters as a function of the mole fraction at constant temperature and thus, from a crystallographic point of view, to account for the lattice deformation due to the substitution process of the guest molecules in the host lattices.

3.2.1. Monoclinic Mixed Crystals. The continuous variation of the lattice parameters vs concentration for the monoclinic phase ($C2/c$, $Z = 32$) at 223.2 K, shown in Figure 5, together with the continuous variation of the temperatures characterizing the [M + R] equilibrium, prove the formation of monoclinic substitutional mixed crystals in the whole composition range. It follows then that the low-temperature phase of $CBrCl_3$ is isomorphous to that of the CCl_4, confirming the structural results found recently for $CBrCl_3$ from neutron powder diffraction on the hypothesis that both compounds were isostructural.[7] In addition, monoclinic lattice parameters of $CBrCl_3$ determined at 223.2 K ($a = 20.620(5)$ Å, $b = 11.613(3)$ Å, $c = 20.195(5)$ Å, $\beta = 111.223(6)°$, and $V/Z = 140.9(1)$ Å^3) agree quite well with those previously published.[7] As for lattice parameters of CCl_4, results agree with those reported in the literature.[14]

To obtain more information about the structure of the monoclinic mixed crystals and, in particular, about the fractional occupancies of the halogen sites, patterns determined at 223.2 K as a function of composition were submitted to a Rietveld profile refinement. First, the process was checked for the pure compound $CBrCl_3$ by using the model detailed by Binbrek et al.[7] Although the set of parameters can be obtained from the work of Binbrek et al., we shortly remember here the basic features of the model. The CBr_4 structure was used as a starting point for the atomic coordinates of the four molecules in the asymmetric unit; fractional occupancies of the halogen sites were set as 0.25 and 0.75 for the Br and Cl atoms, respectively, rigid body representing a pseudomolecule with tetrahedral symmetry in which overlapping Br and Cl atoms located at 1.939 and 1.772 Å from the central carbon atom C (slightly different from those used initially in ref 7), respectively, was used.

The collected and calculated profiles are shown in Figure 6a together with the difference plot between them (the range cutoff is due to the absence of diffraction lines at lower angles and poor signal at higher angles). A similar process was applied to a set of mixed crystals, and the results are shown in parts b and c of Figure 6 for $X = 0.19$ and $X = 0.80$, respectively. The fractional occupancies of the halogen were set according to the composition and attempts to detect partial ordering by varying the fractional occupancies around values of the "perfectly disordered mixed crystal" were unsuccessful.

Although the quality of the fits, as indicated by the R factors as well as by the plotted differences (given in Figure 6), confirms the formation of continuous monoclinic mixed crystals for the whole composition range, the study of a possible ordering as a function of composition is in need of additional measurements that should be carried out by means of some techniques able to describe local order.

3.2.2. OD Mixed Crystals. *Rhombohedral Mixed Crystals.* To obtain the lattice parameters of the R OD mixed crystals, Lindemann capillaries were cooled to the stable low-temperature monoclinic phase and heated again up to 243.2 K to ensure that stable rhombohedral mixed crystals were formed.

Figure 7 shows a 2θ window of the diffraction patterns at 243.2 K for pure components and some representative mixed crystals. The comparison of the patterns as a function of molar composition evidences the appearance of the same reflections enabling thus the pattern of phase II of $CBrCl_3$ to be unambiguously indexed. Additional patterns for phase II of $CBrCl_3$ were measured and after indexing, and lattice parameters were refined at each temperature. Refinement at 204.2 K results in lattice parameters of $a = 14.639(8)$ Å and $\alpha = 89.44(1)°$.

Therefore, the isomorphism between the OD R stable phase Ib of CCl_4 and phase II of $CBrCl_3$ is proved as can be inferred from the continuity of the lattice parameter against concentration (see Figure 8a).

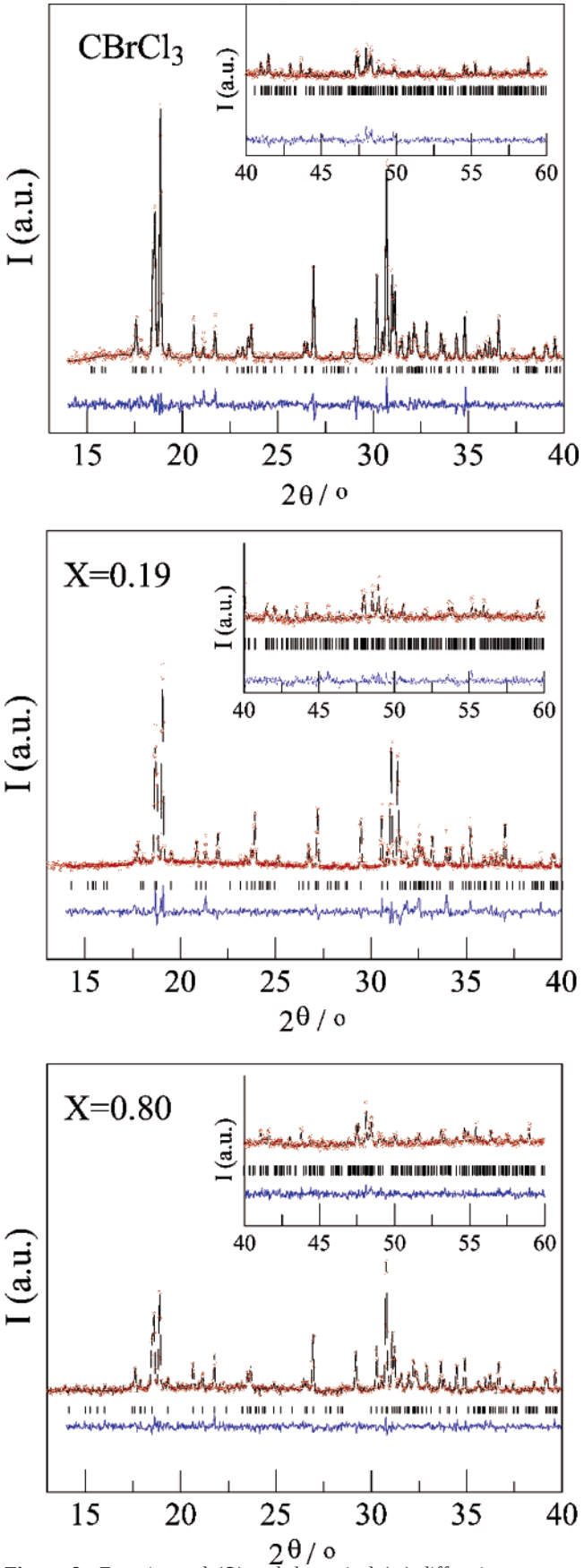

Figure 6. Experimental (○) and theoretical (—) diffraction patterns along with the difference profile of monoclinic phase at 223.2 K for $CBrCl_3$ pure compound ($R_p = 14\%$, $R_{wp} = 18\%$) and $(CCl_4)_{1-X}(CBrCl_3)_X$ mixed crystals with $X = 0.80$ ($R_p = 9.8\%$, $R_{wp} = 7.5\%$) and $X = 0.19$ ($R_p = 11.8\%$, $R_{wp} = 9.2\%$). Each inset corresponds to a four times expanded vertical scale for the data from $2\theta > 40°$.

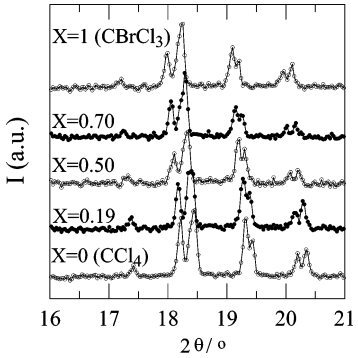

Figure 7. 2θ window of the powder diffraction patterns at 243.2 K for the rhombohedral phase of pure components CCl_4 (lower trace) and $CBrCl_3$ (upper trace) and several mixed crystals (intermediate traces).

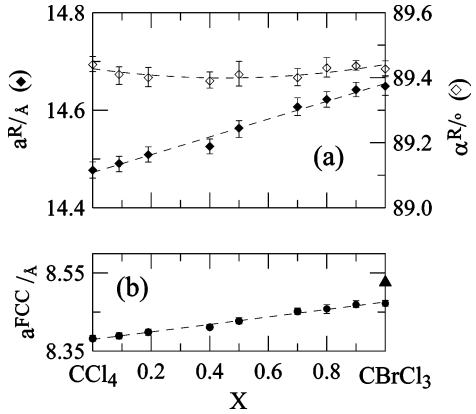

Figure 8. Lattice parameters as a function of the mole fraction for the rhombohedral OD (a) and face-centered cubic (b) mixed crystals at 243.2 K. Triangle corresponds to the lattice parameter of the FCC phase at 262 K given by Binbrek et al.[7]

Face-Centered Cubic Mixed Crystals. From DSC experiments, it has been stated that OD FCC mixed crystals behave either enantiotropically ($1 \geq X \geq 0.80$) or monotropically ($0 \leq X < 0.80$) depending on the composition. However, for both composition domains, they were found persistent enough for their lattice parameters to be determined at 243.2 K (see cooling DSC curves in Figure 3). **Figure 8b** displays the continuous variation of the FCC lattice parameter over the whole concentration range at 243.2 K. This demonstrates the isomorphism relationship between the monotropic FCC phase of CCl_4 and the enantiotropic FCC phase of $CBrCl_3$.

3.3. Thermodynamic Analysis Procedure. *Thermodynamic Formulation.* Under isobaric conditions, the thermodynamic properties of a two-component system are known if for each phase the Gibbs energy of the pure components, as well as the excess Gibbs energy of the mixtures, is known as a function of temperature for the first and as a function of temperature and composition for the second.

The Gibbs energy for a mixture of $(1 - X)$ mol of pure component A and X mol of pure component B displaying isomorphism in the α phase, i.e., the mixed crystal $A_{1-X}B_X$, is connected with the temperature and composition variables by

$$G^{\alpha}(T,X) = (1 - X)\mu_A^{*,\alpha} + X\mu_B^{*,\alpha} + RT\,\mathrm{LN}(X) + G^{E,\alpha}(T,X) \quad (2)$$

in which $\mu_A^{*,\alpha}$ and $\mu_B^{*,\alpha}$ represent the molar Gibbs energies of pure components A and B respectively, R is the gas constant, $\mathrm{LN}(X) = (1 - X)\ln(1 - X) + X \ln X$, and $G^{E,\alpha}(T,X)$ stands for

the excess Gibbs energy that accounts for the deviation of the mixture in form α from ideal mixing behavior.

To determine the two-phase equilibrium region between two phases (α and β) in a two-component phase diagram, the well-known equilibrium rule corresponding to the minimum Gibbs energy of the mixed crystal $A_{1-X}B_X$ at each temperature must be applied, i.e., the common tangent to both Gibbs energies characterizing the phases of the corresponding equilibrium, $G^{\alpha}(T,X)$ and $G^{\beta}(T,X)$ must be determined. To do so, the molar Gibbs energies of the pure compounds A and B as well as the excess properties for each phase are required. In what follows and because of the lack of data on $\mu_i^{*,j}$, i = A and B and $j = \alpha$ and β, the simplified treatment named the equal Gibbs curve (EGC) method was used.[30] The difference between the Gibbs energies of phases α and β can be written as

$$\Delta_{\alpha}^{\beta}G(T,X) = G^{\beta}(T,X) - G^{\alpha}(T,X) = (1-X)\Delta_{\alpha}^{\beta}\mu_{\mathrm{A}}^{*}(T) + X\Delta_{\alpha}^{\beta}\mu_{\mathrm{B}}^{*}(T) + \Delta_{\alpha}^{\beta}G^{\mathrm{E}}(T,X) \quad (3)$$

where $\Delta_{\alpha}^{\beta}\mu_i^{*}(T)$ is $\mu_i^{*,\beta} - \mu_i^{*,\alpha}$ (i = A and B) and $\Delta_{\alpha}^{\beta}G^{\mathrm{E}}(T,X)$ is the excess Gibbs energy difference between the considered phases, i.e., $G^{\mathrm{E},\beta}(T,X) - G^{\mathrm{E},\alpha}(T,X)$.

The equation

$$\Delta_{\alpha}^{\beta}G(T_{\mathrm{EGC}},X) = 0 \quad (4)$$

provides a curve in the $T-X$ plane where the α and β phases have equal values of the Gibbs energies (EGC). By assuming that the heat capacities differences may be ignored, $\Delta\mu_i^{*}(T)$ can be approximately written as $\Delta_{\alpha}^{\beta}S_i^{*}(T_i^{\alpha\rightarrow\beta} - T)$, where $T_i^{\alpha\rightarrow\beta}$ is the temperature of the $\alpha \rightarrow \beta$ transition for the component i, the EGC temperature can be deduced from eq 4 as

$$T_{\mathrm{EGC}} = \frac{(1-X)\Delta_{\alpha}^{\beta}H_{\mathrm{A}}^{*} + X\Delta_{\alpha}^{\beta}H_{\mathrm{B}}^{*}}{(1-X)\Delta_{\alpha}^{\beta}S_{\mathrm{A}}^{*} + X\Delta_{\alpha}^{\beta}S_{\mathrm{B}}^{*}} + \frac{\Delta_{\alpha}^{\beta}G_{\mathrm{EGC}}^{\mathrm{E}}(X)}{(1-X)\Delta_{\alpha}^{\beta}S_{\mathrm{A}}^{*} + X\Delta_{\alpha}^{\beta}S_{\mathrm{B}}^{*}} \quad (5)$$

where $\Delta_{\alpha}^{\beta}H_i^{*}$ and $\Delta_{\alpha}^{\beta}S_i^{*}$ are the enthalpy and entropy change of the $\alpha \rightarrow \beta$ transition for the component i. The first term of the right side of eq 4 represents the EGC temperature for the [α + β] equilibrium when the excess Gibbs energy difference is zero and is only pure-component dependent and thus can be obtained from pure-component data. However, the second term depends on the excess Gibbs energy difference along the EGC curve.

By use of the experimental data at equilibrium [α + β], the mathematical procedure to obtain the excess Gibbs energy difference close to the EGC curve, $\Delta_{\alpha}^{\beta}G^{\mathrm{E}}(X)$, is performed by means of the WINIFIT software,[31] which is a modification in a Windows version of the well-known LIQFIT and PROPHASE programs.[32] In this context, the excess Gibbs energy difference for a given solution is represented by a two-parameter function in the form of a Redlich−Kister polynomial

$$\Delta_{\alpha}^{\beta}G^{\mathrm{E}}(X) = X(1-X)[\Delta_{\alpha}^{\beta}G_1 + \Delta_{\alpha}^{\beta}G_2(1-2X)] \quad (6)$$

where the parameter $\Delta_{\alpha}^{\beta}G_1$ expresses the magnitude of the excess Gibbs energy difference at the equimolar composition and $\Delta_{\alpha}^{\beta}G_2$ gives account for the asymmetry of such a function with respect to $X = 0.5$, both Redlich−Kister parameters having the dimension of energy. It must be stressed that eq 6 provides an excess Gibbs energy difference independent of the temperature and, thus, it means that such a function is representative at temperatures close to the temperature range of the input data.

TABLE 2: $\Delta_{\alpha}^{\beta}G_1$ and $\Delta_{\alpha}^{\beta}G_2$ Parameters of the Redlich−Kister Polynomial for the Excess Gibbs Energy Difference between the Involved Phases in the CCl_4 + $CBrCl_3$ Two-Component System Together with the Equimolar Equal Gibbs Temperature ($T_{\mathrm{EGC}}(X = 0.5)$) for Each of the Assessed Equilibria

equlibrium	α	β	$\Delta_{\alpha}^{\beta}G_1$ (J·mol^{-1})	$\Delta_{\alpha}^{\beta}G_2$ (J·mol^{-1})	$T_{\mathrm{EGC}}(X = 0.5)$ (K)
[R + L]	R	L	−13	−14	264.0
[FCC + L]	FCC	L	−33	−15	255.5
[M + R]	M	R	−92	−74	230.6

Generally, unless the system presents some strong local anomaly, such simple polynomials of two terms are fairly adequate and physically more understandable than other polynomial forms including more than two terms. The next sections describe the thermodynamic analysis results for the two-phase equilibria involved in the two-component system studied in this work.

We conclude this section by the remark that we did not find published excess thermodynamic functions for the liquid mixtures CCl_4 + $CBrCl_3$. Thus, only excess Gibbs energy differences between the ODIC phases, FCC and R, and the liquid state and, consequently, between the monoclinic and the R phases can be obtained.

[FCC + L] Two-Phase Equilibrium. Because of the isomorphism relationship between the metastable FCC phase of CCl_4 and the stable FCC phase of $CBrCl_3$ arising from the continuity of the lattice parameters and the solidus and liquidus temperatures of the [FCC + L] equilibrium, one Gibbs energy can describe thermodynamically the FCC mixed crystals. The temperatures and enthalpy changes corresponding to the FCC melting of the pure compounds (see Table 1), all of them experimentally available, and the temperature data of the equilibrium were used for the thermodynamic assessment using the WINIFIT program. It results in the excess Gibbs energy difference expressed by the Redlich−Kister coefficients given in Table 2.

[R + L] Two-Phase Equilibrium. The extension of the [R + L] loop ends at $X = 1$ at the theoretical metastable melting point of the R phase of $CBrCl_3$, $T_{\mathrm{A}}^{\mathrm{R-L}}$ (see open circle in Figure 1a), which would correspond to the melting temperature of phase R if the FCC phase of $CBrCl_3$ would not exist. The thermodynamic properties of the melting of the R phase of $CBrCl_3$ can be determined by two independent procedures. The first consists of the extrapolation of both temperatures and enthalpy changes of the well experimentally defined [R + L] equilibrium at X = 1. Values obtained in this way are consigned in Table 1. The second way is based on the state of function character of the enthalpy magnitude, which finds expression in the equation $\Delta_{\mathrm{R}}^{\mathrm{L}}\phi(T) = \Delta_{\mathrm{R}}^{\mathrm{FCC}}\phi(T) + \Delta_{\mathrm{FCC}}^{\mathrm{L}}\phi(T)$, where $\phi \equiv H,S$, assuming that contributions of the specific heat are small to have a noticeable influence in the narrow temperature domain. Such a procedure provides values with a difference smaller than 1.5% for the melting enthalpy and entropy of the R phase. It should be noticed that the agreement between both procedures enhances the quality of the experimental data as well as the validity of the previous assumption passing over the heat capacities for a narrow temperature domain.

With the melting thermodynamic properties of the R phase for both pure compounds and the [R + L] temperature data, the thermodynamic analysis provides the excess Gibbs energy difference between R and L phases gathered in Table 2.

[R + FCC] Two-Phase Equilibrium. In contrast to the wealth of information available on melting temperature and

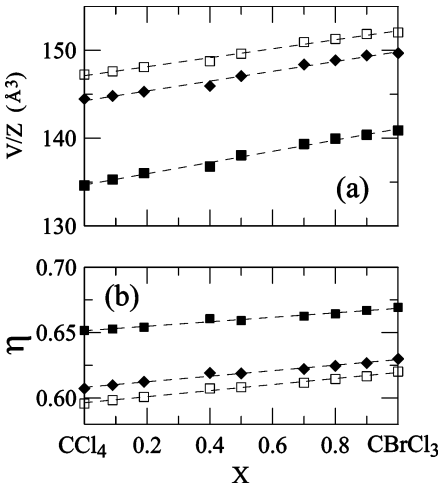

Figure 9. Volume occupied by a molecule (a) and packing coefficient (b) of the monoclinic (■), at 223.2 K, and R (♦) and FCC (□), at 243.2 K, mixed crystals.

enthalpy values, little appears to be known about the R to FCC transition for mixed crystals with molar composition range between $X = 0$ (CCl_4) and $X = 0.80$. Thus, in the case of the [R + FCC] equilibrium, the procedure is less straightforward because the thermodynamic properties of the metastable transition point of CCl4 (see $T_B^{R\rightarrow FCC}$ in Figure 1b) are not known and because of the very narrow composition domain occupied by the [R + FCC] equilibrium in the $CBrCl_3$-rich composition side. By applying the thermodynamic relations based on the state of function character of the enthalpy and entropy properties described in the preceding paragraph, the fundamental properties of the virtual transition R to FCC were obtained.

[M + R] Two-Phase Equilibrium. Pure-component data for the M to R transition compiled in Table 1, along with the solvus temperatures as a function of composition, were used to infer the excess Gibbs energy difference between the aforementioned phases. The polynomial coefficients for such a difference are gathered in Table 2.

The complete phase diagram resulting from the described thermodynamic assessment together with the experimental values is shown in Figure 2. This figure includes also, as a superposition in Figure 2a, the metastable part of the [FCC + L] equilibrium. As can be seen, experimental and calculated equilibria match up, the maximum temperature deviation being within the experimental uncertainties of the measured temperatures.

The temperature of the peritectic invariant is determined to be 262.4 K, and the mole fractions characterizing the three-phase equilibrium are 0.796, 0.802, and 0.807.

At first sight, the results of the approach are evidence that R, FCC, and L phases show almost the same deviation with regard to the ideal mixing behavior, an experimental result that is commonly found for OD mixed crystals. As far as low-temperature monoclinic mixed crystals are concerned, it should be noted that the excess Gibbs energy difference with respect to the OD R phase is relatively small when compared with other similar systems.[33−35]

4. Discussion

The crystallographic study enables us to calculate the variation of the volume occupied by a molecule for each one of the explored mixed crystals as a function of molar composition (see Figure 9a). Such a value can be used to determine the variation of the packing coefficient $\eta(X)$ in order to extract information about the packing differences when species of the same chemical nature are arranged in a different translational and orientational order, because the introduction of a foreign molecule in a lattice, giving rise to mixed crystals, modifies the molecular surroundings and influences the intermolecular interactions governing the thermodynamic and structural properties.

The packing coefficient is defined as $\eta = V_m/(V/Z)$, where V_m is the molecular volume, V is the unit-cell volume, and Z is the number of molecules in the unit cell. The molecular volumes of the pure components were computed using the values of the van der Waals radii and interatomic chemical bonds following Kitaigorodsky's method.[36] The van der Waals volumes are 87.72 and 94.29 Å^3 for CCl_4 and $CBrCl_3$, respectively. A very simple way to determine the packing of the mixed crystals is to set for a mixed crystal of molar composition X, as a linear contribution of the molecular volumes of the molecules taking part in the mixed crystal, i.e., $V_m(X) = (1 - X)V_m(CCl_4) + XV_m(CBrCl_3)$. The resulting values for the packing coefficient as a function of the molar composition for each kind of mixed crystals are shown in Figure 9b. As we can observe, the highest packing corresponds to the low-temperature monoclinic phase, in accordance with the well-known rule that the most favorable packing of molecules in a crystal has the strongest interactions and hence the greatest density. Similarly, results evidence that the packing of the OD R mixed crystals is higher than that of the OD FCC mixed crystals (both measured at the same temperature, 243.2 K) whatever the composition, i.e., in the region in which FCC mixed crystals behave monotropically with respect to R mixed crystals ($0 < X < 0.80$) and in the region in which the FCC mixed crystals have been metastabilized at 243.2 K. It must be noticed that it is usually accepted that, when comparing two phases experimentally accessible at the same temperature, the most stable structure must display the highest packing ("close-packing principle").[36]

As a conclusion, there is a good agreement between these crystallographic results and the stability domains of the phases involved in the phase diagram. In addition, it should be stressed that the molar volume against molar composition for the whole analyzed phase is almost linear, which means that the excess volume is negligible, in accordance with the small excess thermodynamic properties derived from the thermodynamic assessment.

Noteworthy is the relatively small excess Gibbs energy difference between the R and the M phases. Accordingly, this value should correspond to the well-known manifestation of a similarity between the host and guest molecules as well as the intermolecular interactions (taking into consideration that excess enthalpy seems to be small, see Figure 4) and the additional disorder introduced by the substitution process. It has been well established that, for mixed crystals formed between compounds in which orientational and translational long-range order exists, the molecular symmetry appears to be of crucial importance.[37,38] If the steric conditions permit the molecular substitution of the guest molecule in the host lattice and the guest molecule does not display the required symmetry elements of the host lattice site, a symmetry simulation must be generated by the appearance of an orientational disorder or by a change of the occupancy of the sites when the molecules are very close in shape. This obvious requirement has been argued to explain the large miscibility in the OD phases.[38−40] For the analyzed monoclinic mixed crystals, although the molecular symmetry of the CCl_4 molecules (T_d) is higher than that of the $CBrCl_3$ molecules (C_{3v}), the T_d symmetry should be fulfilled by the latter, because the lattice symmetry of both monoclinic phases of pure compounds

have been found to be one and the same ($C2/c$). In fact, the authors of the recent work reporting the structure of the low-temperature phase for $CBrCl_3$ point out the impossibility to detect any ordering of the molecules by varying the fractional occupancy of the halogen sites,[7] thus indicating the existence of a disorder whatever the analyzed temperature (from 5 to 250 K). Nevertheless, the study of the heat capacity[6] pointed out the existence of a glass transition at around 90 K associated with the freezing of the exchange positions between Cl and Br atoms. The existence of such a glass transition means that, below 90 K, the system falls into a nonequilibrium state (despite the fact that the authors did not report a value for the residual entropy at 0 K) and thus that the transition to a plausible additional phase at a lower temperature, in which the Cl and Br atoms occupy defined site positions, is missing.[41] In this framework, it is quite reasonable to assume that the samples used for neutron diffraction were in the same conditions at temperatures lower than 90 K, i.e., in the nonergodic state corresponding to the ergodic phase II in which Cl and Br atoms are disordered and then the reported structure at temperatures lower than 90 K should correspond to the frozen monoclinic phase II. The linear dependence of the lattice parameters of the monoclinic mixed crystals with the mole fraction together with the small excess Gibbs energy difference determined from the thermodynamic analysis of the [M + R] equilibrium reinforce the disorder concerning the Cl and Br atoms in the $CBrCl_3$ compound.

5. Conclusions

Calorimetric and X-ray powder diffraction techniques have been used to determine the stable phase diagram between CCl_4 and $CBrCl_3$ compounds as well as the metastable two-phase equilibria. The monotropic character of the R to FCC transition of CCl_4 gives rise to a partially metastable [FCC + L] equilibrium in such a way that also the R to FCC transition behaves monotropically for the mixed crystals. In addition, a complete thermodynamic analysis was performed to reproduce the monotropic behavior as well as the stable phase diagram. Such an analysis enables the determination of the thermodynamic properties concerning the nonexperimentally available transition of pure compounds, especially for the R to FCC transition of CCl_4 and for the melting of the rhombohedral phase of $CBrCl_3$. Therefore, this study goes beyond the experimental determination of a phase diagram between two compounds displaying OD phases.

On the other hand, the study enables us to conclude the isomorphism between the OD phases: (i) between the R phase Ib of CCl_4 and R phase II of $CBrCl_3$ and (ii) between the FCC phase Ia of CCl_4 and FCC phase I of $CBrCl_3$ as well as between the low-temperature monoclinic phases (phase II of CCl_4 and phase III of $CBrCl_3$) of the pure compounds. It is worth noting that such a finding results in a direct determination of the lattice symmetry of the OD R phase of $CBrCl_3$, which was unsolved from previous neutron diffraction works.

As for the low-temperature phase of $CBrCl_3$, further structural studies analyzing the disorder induced by fractional occupancy of the sites occupied by the Cl and Br atoms would be interesting. In respect to this problem, it is quite possible that a "missing" low-temperature phase of $CBrCl_3$, with translational and orientational long-range order, can be nonexperimentally available, in such a way that the mixed crystals obtained in this work could be the only path to characterize it through the analysis of the structural properties as a function of the mole fraction and thus for a better insight into the dynamics of supercooled glassforming in which the occupancy of several atoms in the molecular structure constitutes the frozen disorder.[42]

Acknowledgment. This work was supported by the Spanish Ministry of Science and Technology under project BFM2002-01425 and by the Catalan government by the grant SGR2002-00152. One of us, M.B., acknowledges the financial support of the Catalan government for the fellowship 2002BEIA400207.

References and Notes

(1) Miller, R. C.; Smyth, C. P. *J. Chem. Phys.* **1956**, *24*, 814.
(2) Miller, R. C.; Smyth, C. P. *J. Am. Chem. Soc.* **1957**, *79*, 20.
(3) Chihara, H.; Shinoda, T. *Bull. Chem. Soc. Jpn.* **1964**, *37*, 125.
(4) Anderson, A.; Torrie, B. H.; Tse, W. S. *Chem. Phys. Lett*. **1979**, *61*, 119.
(5) Timmermmans, J. *J. Chim. Phys*.**1938**, *35*, 331.
(6) Ohta, T.; Yamamuro, O.; Matsuo, T. *J. Phys. Chem.* **1995**, *99*, 2403.
(7) Binbrek, O. S.; Lee-Dadswell, S. E.; Torrie, B. H.; Powell, B. M. *Mol. Phys*. **1999**, *96*, 785.
(8) Lee-Dadswell, S. E.; Torrie, B. H.; Binbrek, O. S.; Powell, B. M. *Physica B* **1998**, *241*−*243*, 459.
(9) Rudman, R. *J. Chem. Phys*. **1977**, *66*, 3139.
(10) Silver, L.; Rudman, R. *J. Phys. Chem*. **1970**, *74*, 3134.
(11) Rudman, R.; Post, B. *Mol. Cryst*. **1968**, *5*, 95.
(12) Rudman, R. *Solid State Commun.* **1979**, *29*, 785.
(13) Powers, R.; Rudman, R. *J. Chem. Phys.* **1980**, *72*, 1629.
(14) Cohen, S.; Powers, R.; Rudman, R. *Acta Cryst*. **1979**, *B35*, 1670.
(15) Powers, R.; Rudman, R. *J. Chem. Phys.* **1980**, *72*, 1629.
(16) More, M.; Baert, F.; Lefevre, J. *Acta Cryst*. **1977**, *B33*, 3681.
(17) Dolling, G.; Powell, B. M.; Sears, V. F. *Mol. Phys.* **1979**, *37*, 1859.
(18) Rudman, R.; Post, B. *Science* **1966**, *154*, 1009.
(19) Koga, Y.; Morrison, J. A. *J. Chem. Phys.* **1975**, *62*, 3359.
(20) Morrison, J. A.; Richards, E. L.; Sakon, M. *J. Chem. Thermodyn.* **1976**, *8*, 1033.
(21) Arentsen, J. G.; Miltenburg, J. C. *J. Chem. Thermodyn.* **1972**, *4*, 789.
(22) Hicks, J.; Hooley, J.; Stephenson, J. G. *J. Am. Chem. Soc*. **1944**, *66*, 1064.
(23) Rudman, R. *J. Mol. Struct*. **2001**, *569*, 157.
(24) Pardo, L. C.; Barrio, M.; Tamarit, J. Ll.; López, D. O.; Salud, J.; Negrier, P.; Mondieig, D. *Chem. Phys. Lett***. 1999**, *308*, 204.
(25) Pardo, L. C.; Barrio, M.; Tamarit, J. Ll.; López, D. O.; Salud, J.; Negrier, P.; Mondieig, D. *Chem. Phys. Lett.* **2000**, *321*, 438.
(26) Pardo, L. C.; Barrio, M.; Tamarit, J. Ll.; López, D. O.; Salud, J.; Negrier, P.; Mondieig, D. *Phys. Chem. Chem. Phys*. **2001**, *3*, 2644.
(27) Ballon, J.; Comparat, V.; Pouxe, J. *Nucl. Instrum. Methods* **1983**, *217*, 213.
(28) Evain, M.; Deniard, P.; Jouanneaux, A.; Brec, R. *J. Appl. Cryst.* **1993**, *26*, 563.
(29) Rodríguez-Carvajal, J. *AFMAIL*; Laboratoire Leon Brillouin, CEA-CNRS: France, 1985.
(30) Oonk, H. A. J. *Phase Theory*: *The Thermodynamics of Hetereogeneous Equilibria*; Elsevier Science Publishers: Amsterdam, 1981.
(31) Daranas, D.; López, R.; López, D. O. *WINIFIT 2.0*.; Polythecnic University of Catalonia, 2000.
(32) Jacobs, M. H. G.; Oonk, H. A. J. *LIQFIT*. A computer program for the Thermodynamic Assessment of T−X Liquidus or Solidus Data. Utrecht University, 1990.
(33) Pardo, L. C.; Barrio, M.; Tamarit, J. Ll.; López, D. O.; Salud, J.; Negrier, P.; Mondieig, D. *J. Phys. Chem. B,* **2001**, *105*, 10326.
(34) López, D. O.; van Braak, J.; Tamarit, J. Ll.; Oonk, H. A. J. *Calphad* **1994**, *18*, 387.
(35) Chellappa, R.; Chandra, D. *Calphad* **2003**, *27*, 133.
(36) Kitaigorodsky, A. I. *Mixed Crystals*; Springer-Verlag: Berlin, 1984.
(37) Haget, Y.; Chanh, N. B.; Meresse, A.; Bonpunt, L.; Michaud, F.; Negrier, P.; Cuevas-Diarte, M. A.; Oonk, H. A. J. *J. Appl. Cryst.* **1999**, *32*, 481.
(38) Barrio, M.; López, D. O.; Tamarit, J. Ll.; Negrier, P.; Haget. Y. *J. Mater. Chem.* **1995**, *5*, 431.
(39) Barrio, M.; López, D. O.; Tamarit, J. Ll.; Negrier, P.; Haget. Y. *J. Sol. State Chem***. 1996**, *124*, 29.
(40) Tamarit, J. Ll.; Barrio, M.; López, D. O.; Haget, Y. *J. Appl. Cryst*. **1997**, *30*, 118.
(41) Suga, H.; Seki, S.; *J. Non-Cryst. Solids* **1974**, *16*, 171.
(42) Höchli, U. T.; Knorr, K.; Loidl, A. *Adv. Phys.* **1990**, *39*, 405.